

ПРОТОННАЯ РАДИОГРАФИЯ ПЛОТНОЙ ПЛАЗМЫ

В.И. Туртиков, А.А. Голубев, К.Л. Губский, В.С. Демидов, А.В. Канцырев, А.П. Кузнецов, Г.Н. Смирнов,
Л.М. Шестов, А.Д.Фертман, Б.Ю. Шарков
ИТЭФ, Москва

С.А. Колесников, С.В. Дудин, В.В. Лавров, В.Б. Минцев, А.В. Савченко, А.В. Уткин, К.А.Бабочкин,
Н.С. Шилкин, Д.С.Юрьев, В.Я.Терновой, Д.Н.Николаев, В.Е. Фортов
ИПХФ РАН, Черноголовка

В.В.Бурцев, Н.В.Завьялов, А.Л.Михайлов, С.А. Картанов, А.В.Руднев, М.В.Таценко
РФЯЦ ВНИИЭФ, Саров

Proton Radiography of Dense Plasma

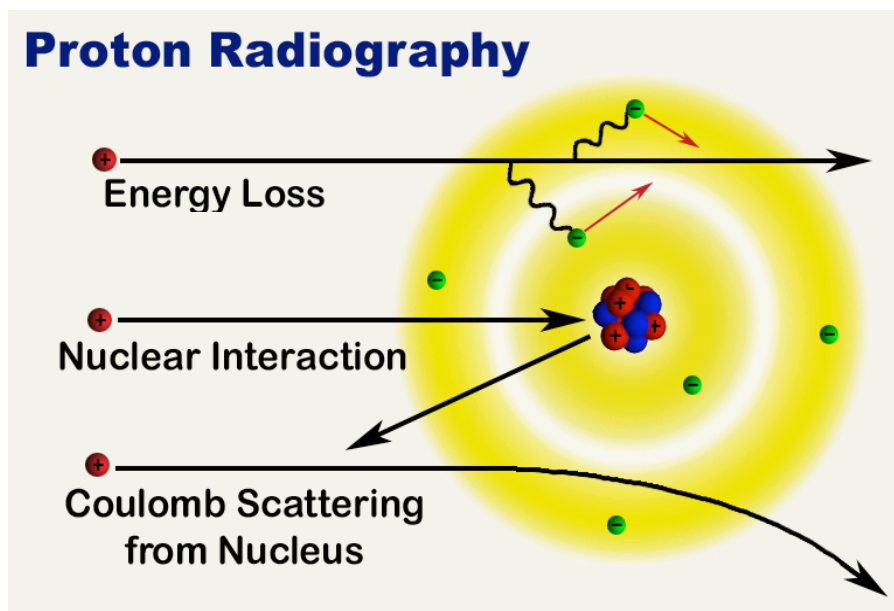
V.I. Turtikov, A.A. Golubev, K.L. Gubskyi, V.S. Demidov, A.V. Kantsyrev, A.P. Kuznetzov, G.N.Smirnov,
L.M.Shestov, A.D. Fertman, B.Yu. Sharkov
Institute for Theoretical and Experimental Physics, Moscow, Russia

S.A. Kolesnikov, S.V. Dudin, V.V. Lavrov, V.B. Mintsev, A.V. Savchenko, A.V. Utkin, K.A. Babochkin,
N.S. Shilkin, D.S.Yuriev, V. Ya.Ternovoi, D.N. Nikolaev, V.E. Fortov
Institute of Problems of Chemical Physics, Chernogolovka, Russia

V. V. Burtsev, N.V. Zavjalov, A. L. Mikhailov, S. A. Kartanov, A. V. Rudnev, M. V. Tatsenko
All-Russia Research Institute of Experimental Physics, Russian Federal Nuclear Center, Sarov, Russia

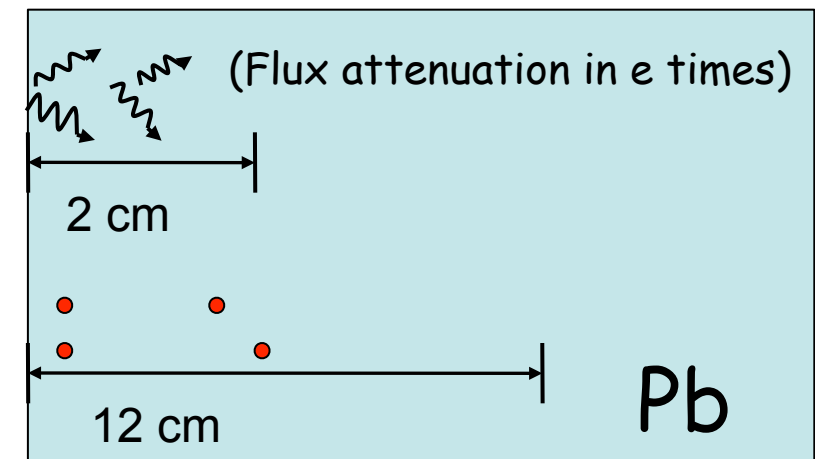
Proton Radiography Basics

X-rays and protons ranges in matter



X-rays 3-10 MeV

High Energy Protons ~ GeV



Protons Image Blurring due to MCS

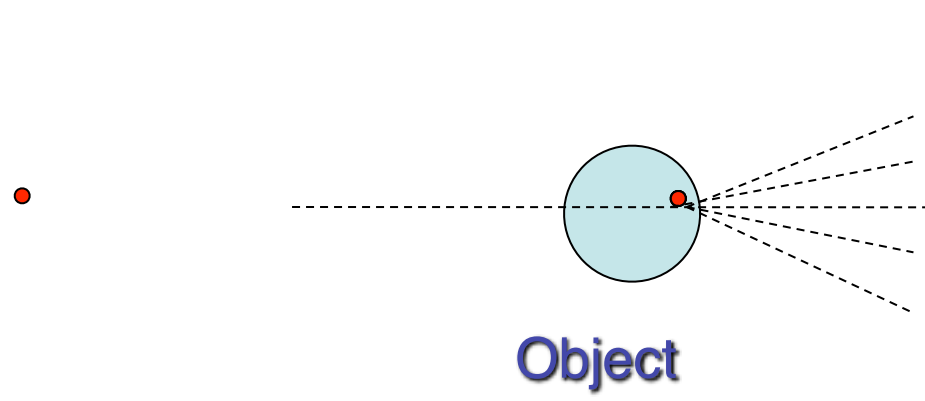
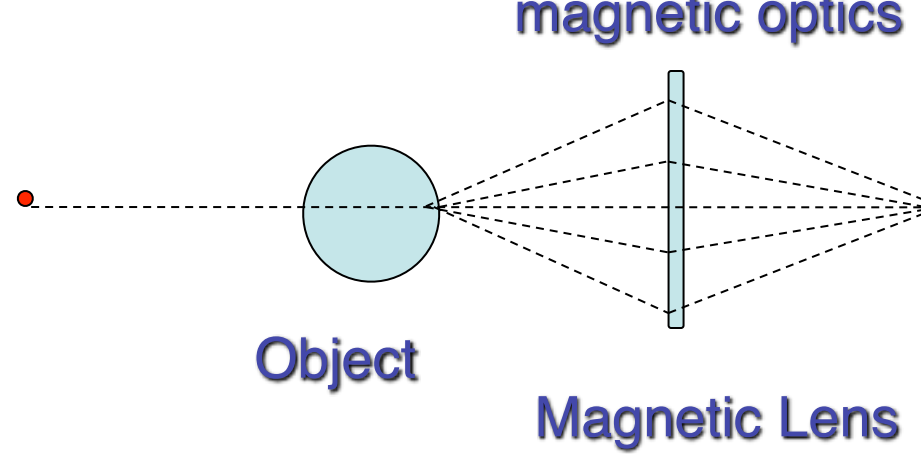


Image Blurring compensation with magnetic optics



A. M. Koehler, et al. Science 160, 303 (1968)

J. A. Cookson Naturwissenschaften 61, 184–191 (1974)

C.L. Morris, J.D. Zumbro, Overview of proton radiography—concepts and techniques, Technical Report LA-UR-97-4172, Los Alamos National Laboratory, 1997.

Proton Radiography Set-up at ITEP-TWAC Facility



ITEP Proton Microscope

$E = 800 \text{ MeV}$

Beam structure – 4 bunches

10^{11} protons

Magnification $X = 7.82$

Field of view $< 10\text{mm}$

Spatial resolution $\sigma = 50\mu\text{m}$

Magnification $X = 3.65$

Field of view $< 22 \text{ mm}$

Spatial resolution $\sigma = 60\mu\text{m}$

Density resolution $\sim 6\%$

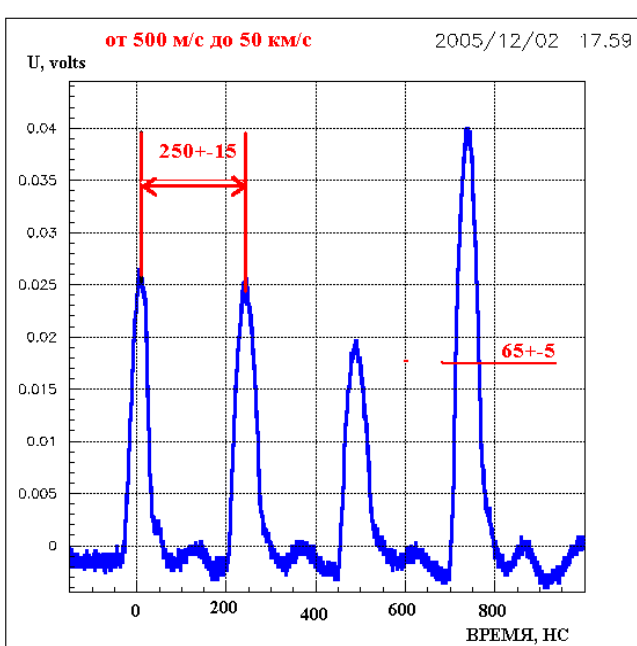


Image Registration System

LSO (40 ns) scintillating converter $\varnothing 78 \text{ mm}$

14 bit CCD camera with fast shutter (100 ns)
matched to beam bunch

Fast Current Transformer (FCT) -
beam intensity measurements;
beam bunch matching



Explosion Protective Chamber

HE mass (TNT) – up to 70 g

Pumped down to 10^{-3} Torr

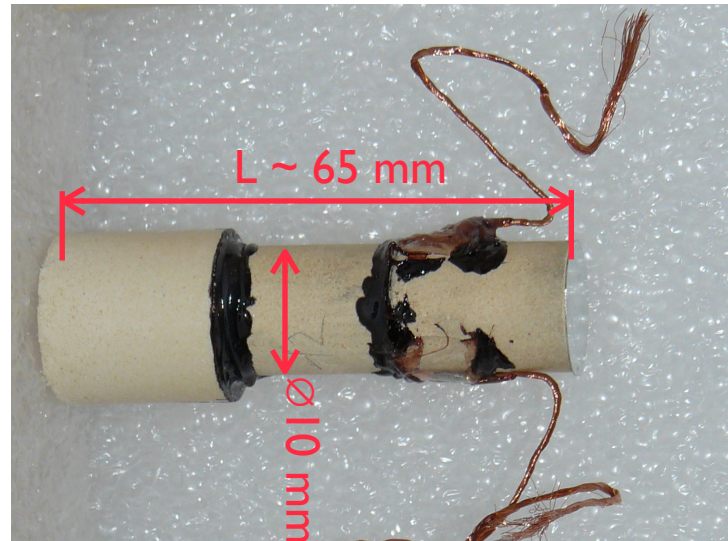
Active ventilation system

Optical diagnostics - VISAR

Under design:

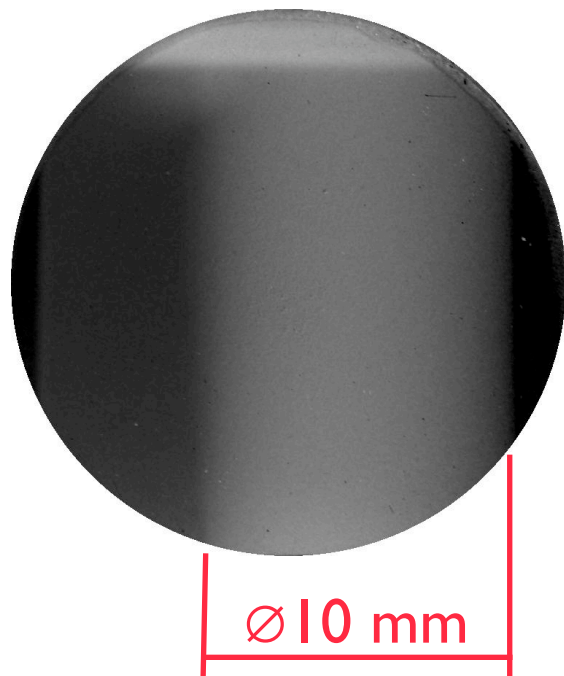
target angular positioning system ($\pm 10^\circ$)
cryogenic target system

Detonation studies in pressed TNT charge

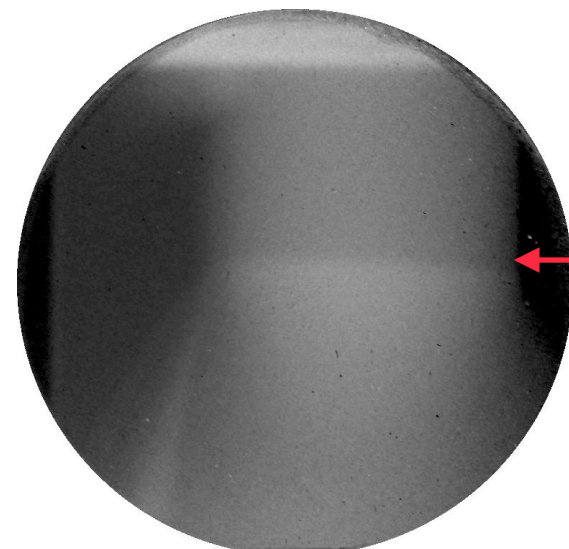


total HE charge weight	25g
initial density	1.32 - 1.65 g/cc
charge diameter	10; 15; 20 mm
charge length	30-56 mm

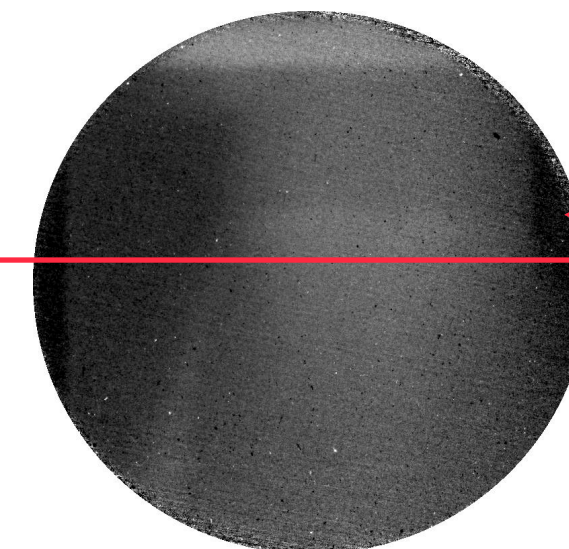
Static image



Bunch 2 image (T_2)



Bunch 3 image (T_3)

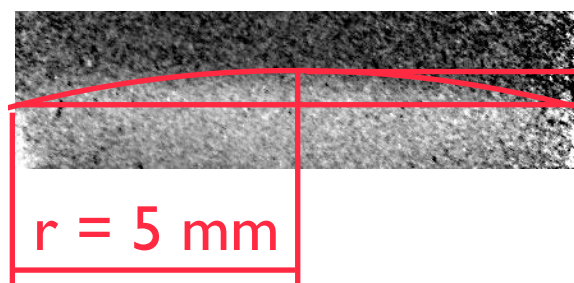


$$\Delta T = T_3 - T_2 = 250 \text{ ns}$$

$$\delta T = 70 \text{ ns}$$

$$\Delta X = 1.72 \pm 0.05 \text{ mm}$$

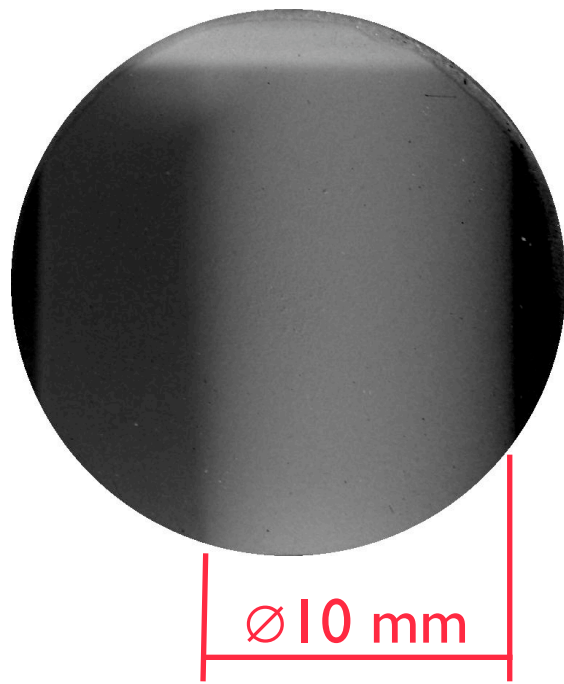
$$\text{Detonation velocity } D = \Delta X / \Delta T = 6.9 \pm 0.2 \text{ km/s}$$



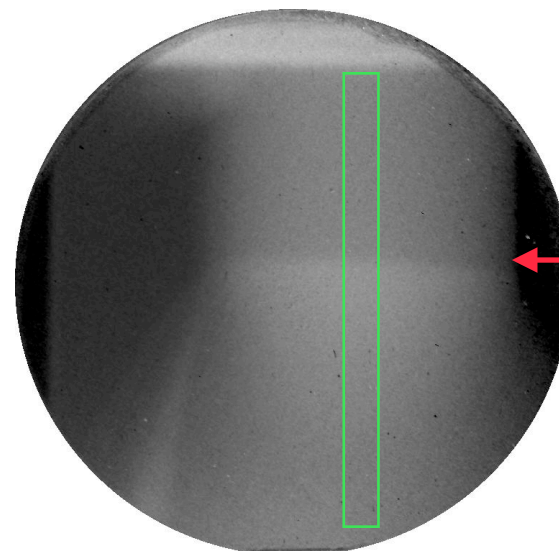
$$\text{Detonation front curvature radius } R = 58 \pm 7 \text{ mm}$$

Detonation studies in pressed TNT charge

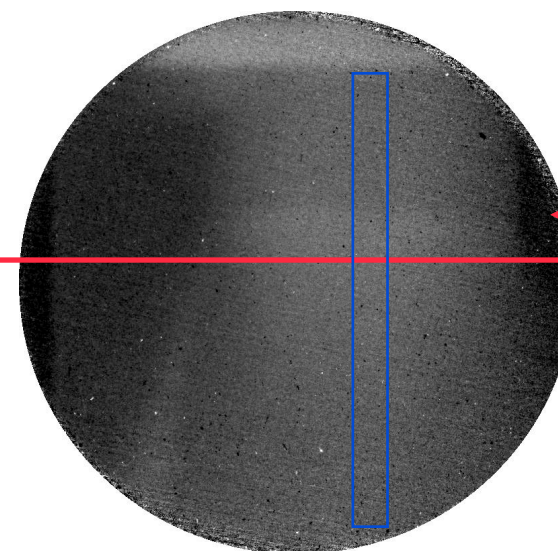
Static image



Bunch 2 image (T_2)



Bunch 3 image (T_3)



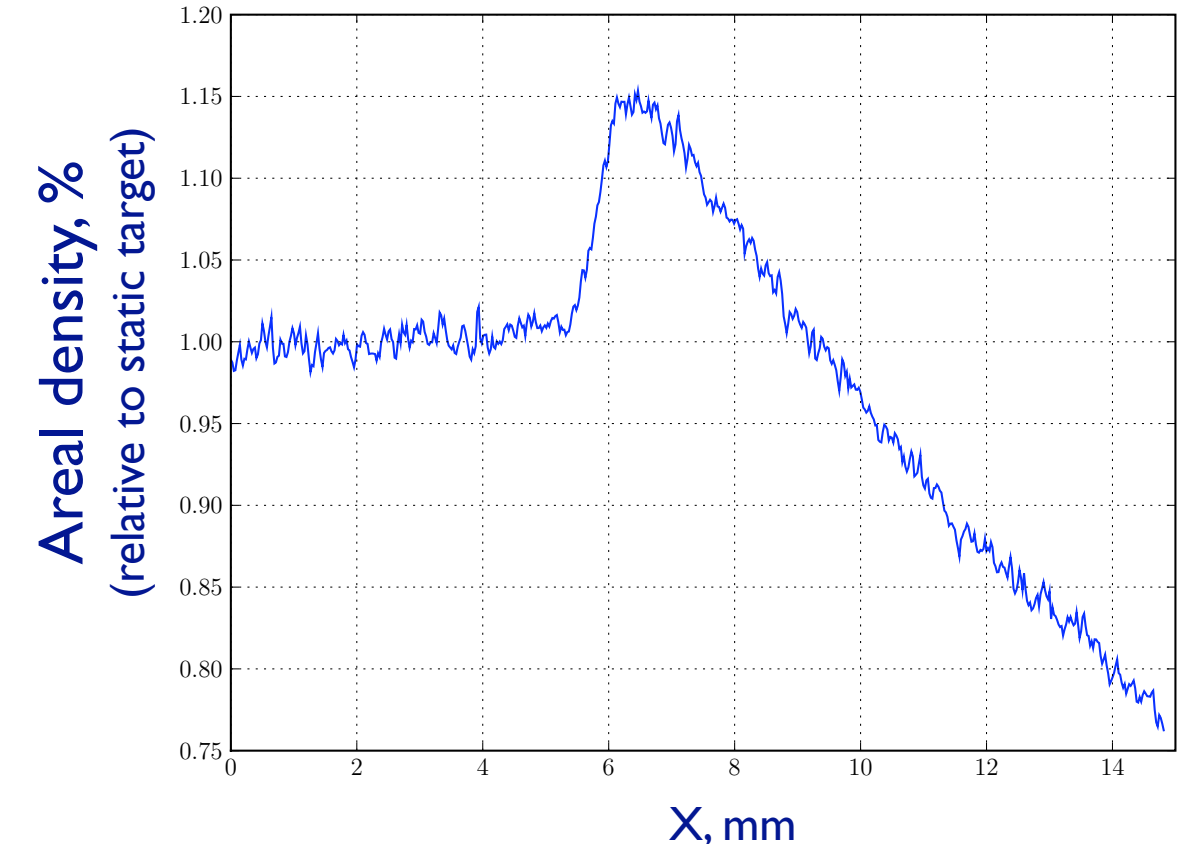
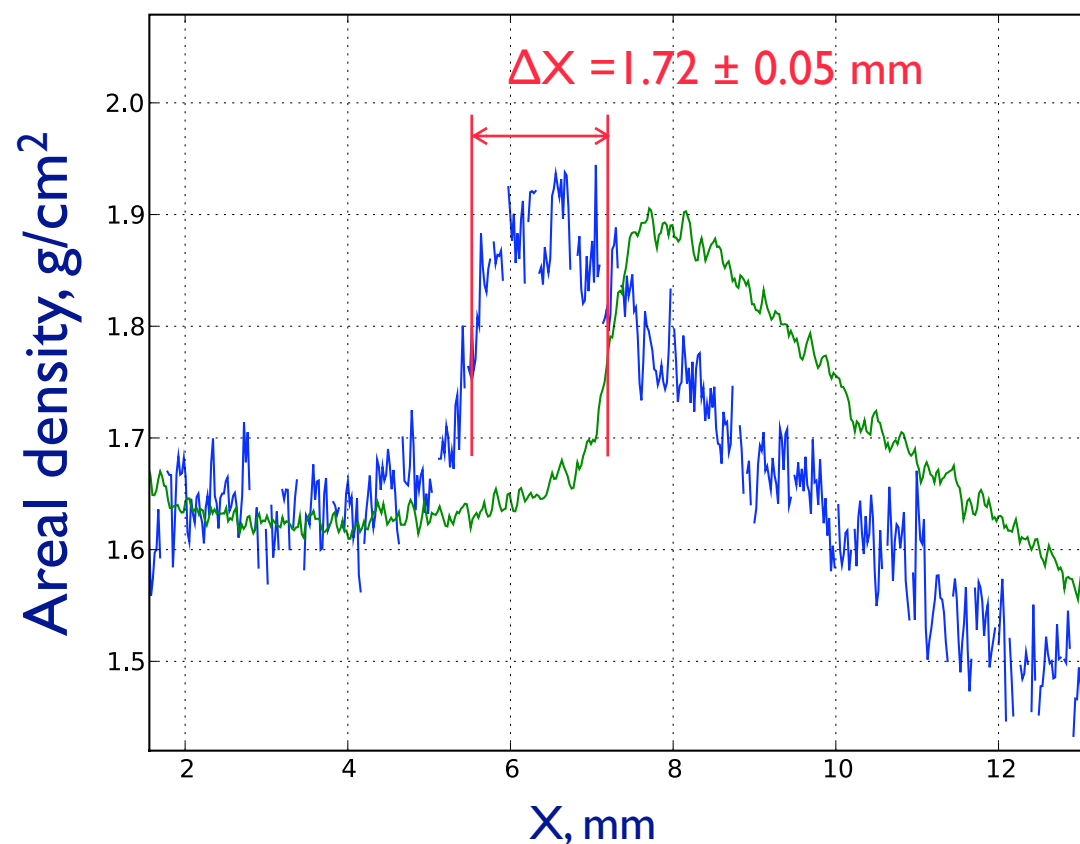
$$\Delta T = T_3 - T_2 = 250 \text{ ns}$$

$$\delta T = 70 \text{ ns}$$

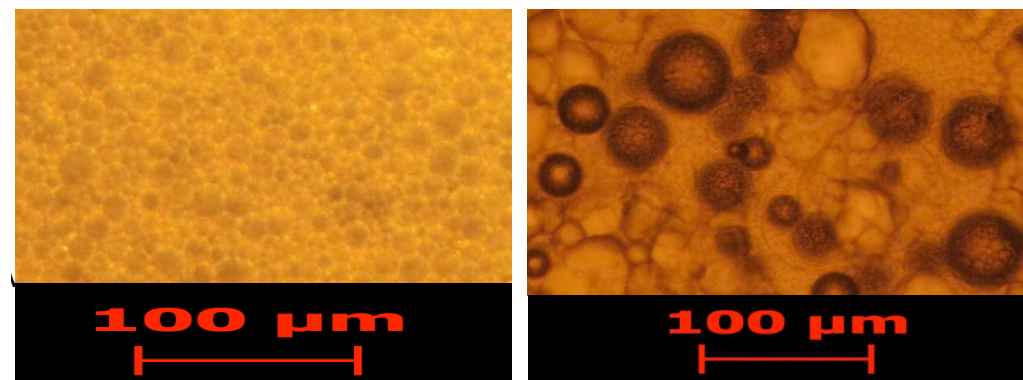
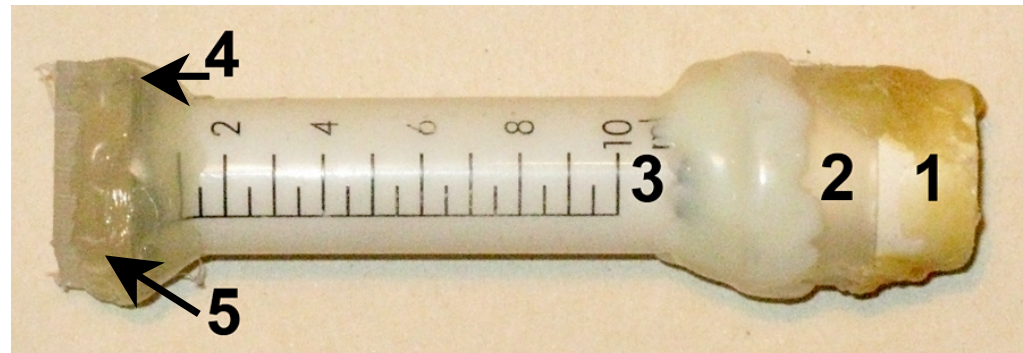
$$\Delta X = 1.72 \pm 0.05 \text{ mm}$$

$$D = \Delta X / \Delta T = 6.9 \pm 0.2 \text{ km/s}$$

Motion blur $\delta X = D\delta T = 0.48 \text{ mm} !$

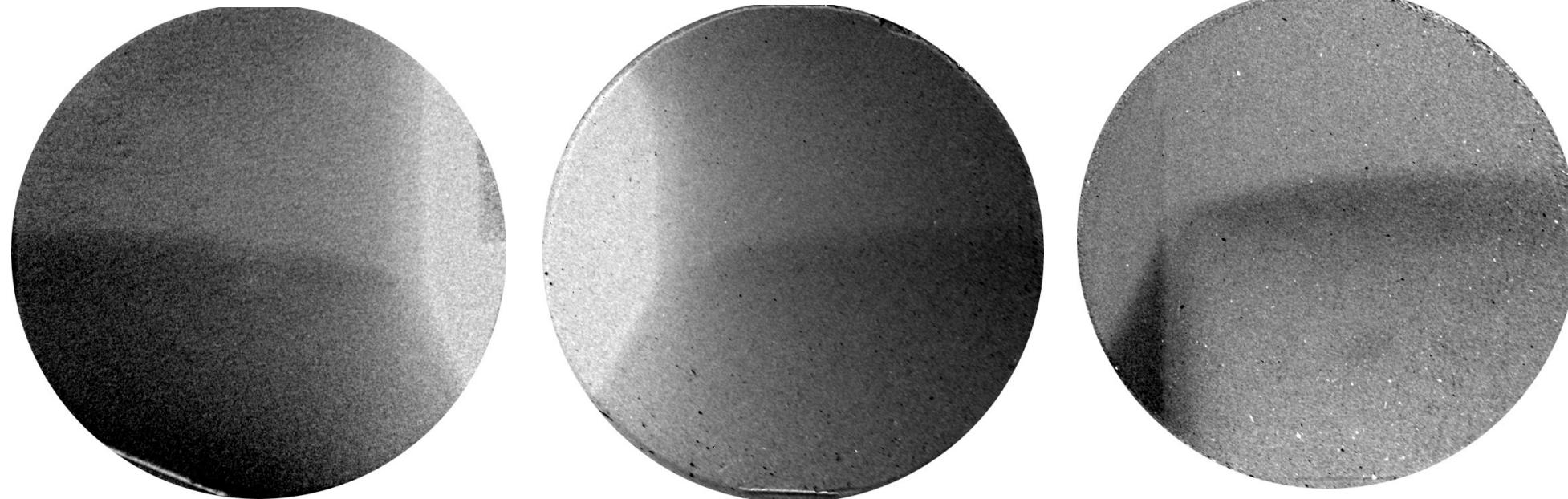


Detonation studies of Emulsion Explosive



92-95% - oxidizer (ammonium nitrate)	
8-5% - fuel (mineral oil)	
Hollow glass microballoons (C15-type, 3M)	
Weight concentration: 1—4%	
density	1.07 g/cc
charge diameter	15; 20 mm
charge length	30-56 mm

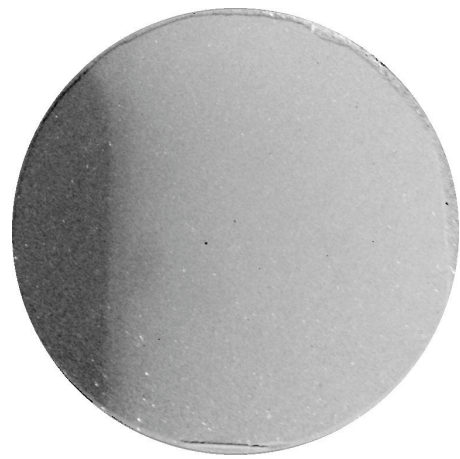
Radiography Images of EHE



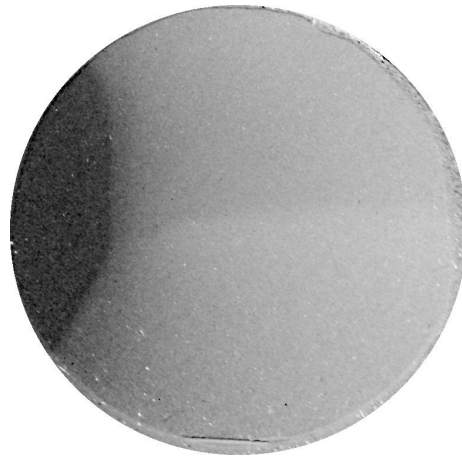
Detonation velocity $D = 4.6 \pm 0.2 \text{ km/s}$

Detonation studies of Emulsion Explosive

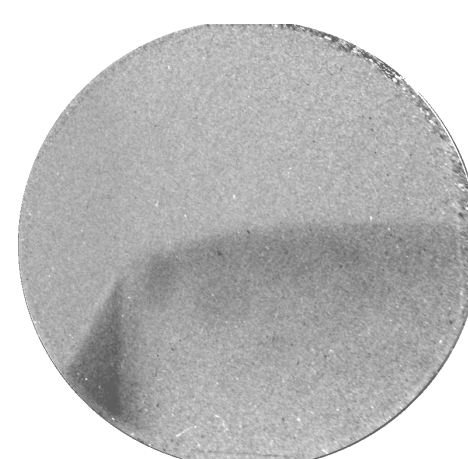
Static image



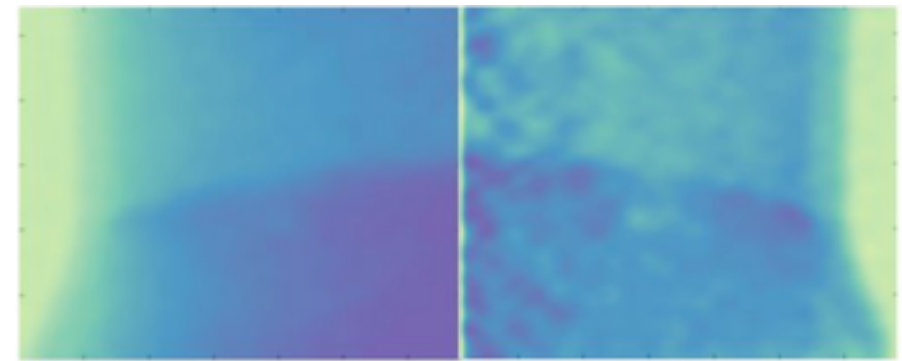
Shot image
(bunch I)



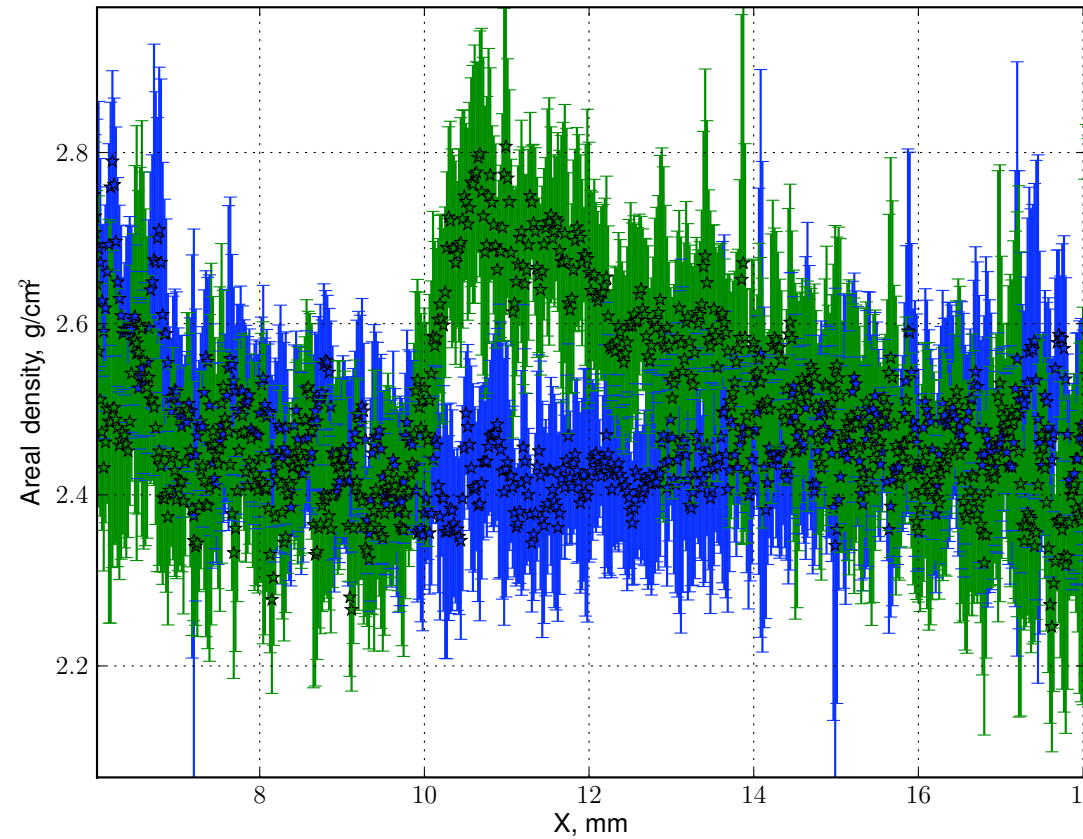
Relative to static
density changes



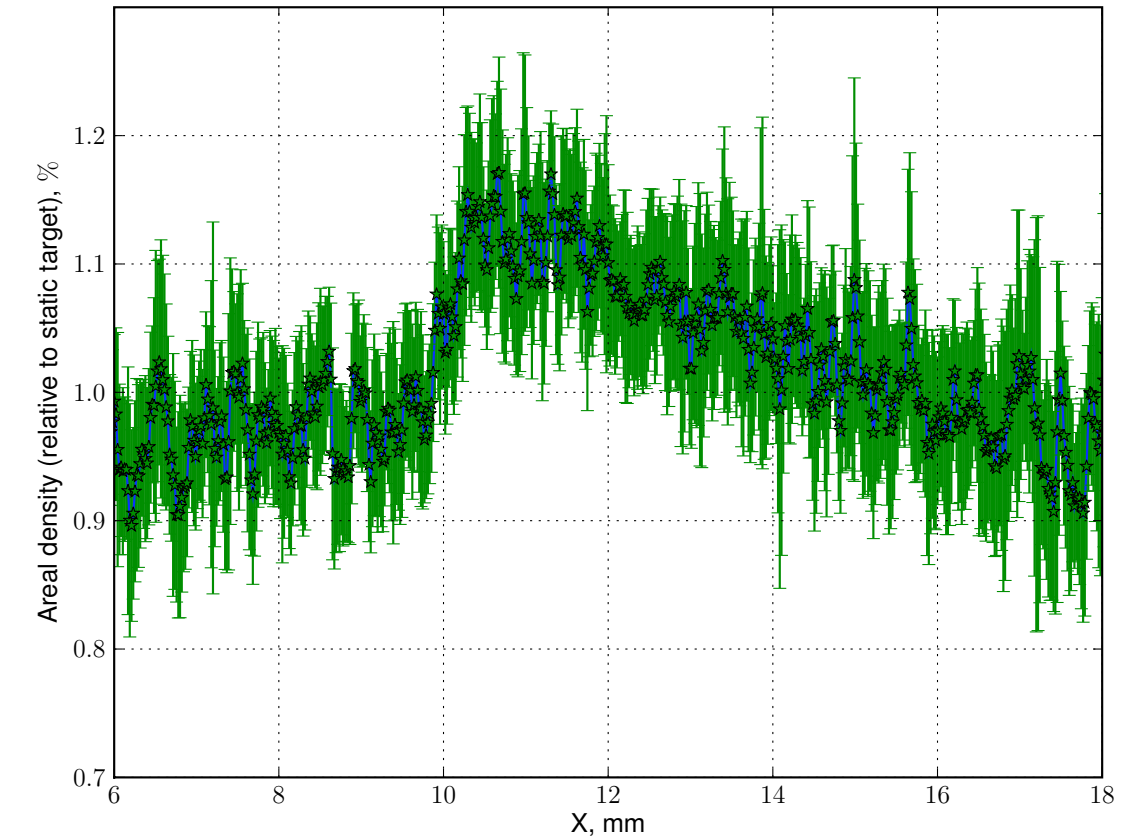
Volume density reconstruction



Areal density profile along charge

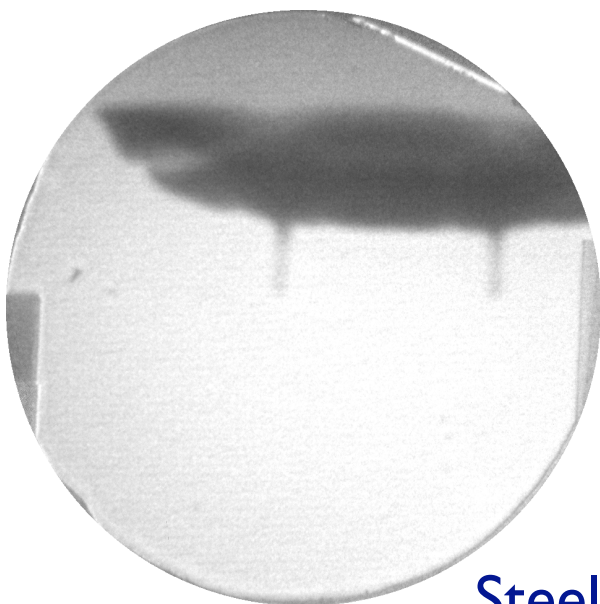


Areal density profile along charge
(relative to static density)

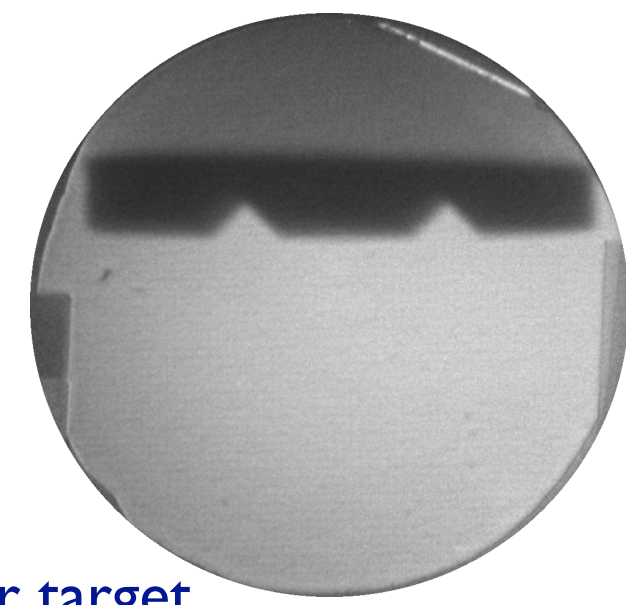


Dynamic Fracture and Surface Ejecta Formation of Metals under Shock Loading

Proton radiography image of dynamic shot at 2.5 μ s after coming of the shock wave to the free surface of the target

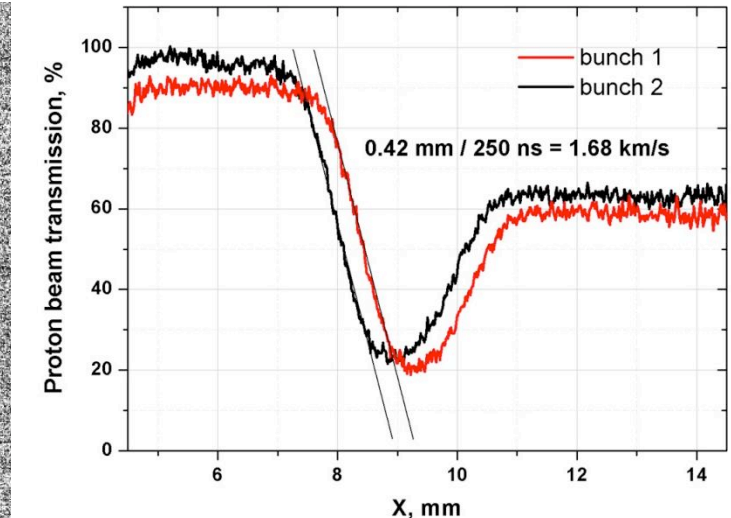
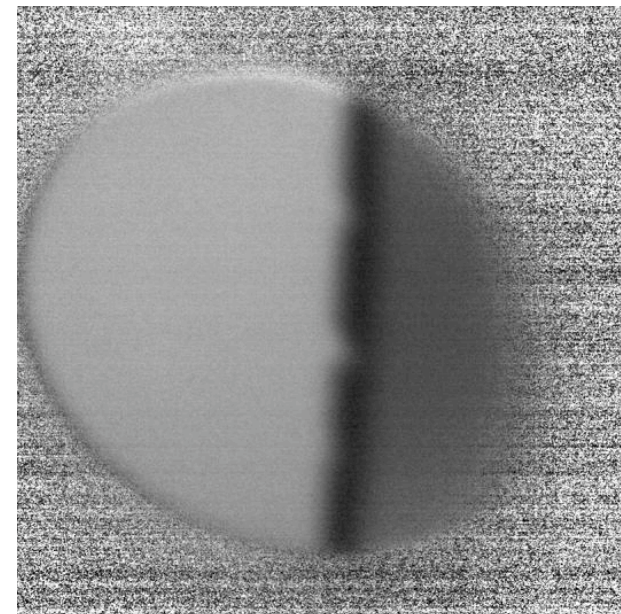


Steel target



Copper target

1 mm thick steel plate with 0.3 and 0.5 mm deep triangular cuts placed on the face of the TNT charge

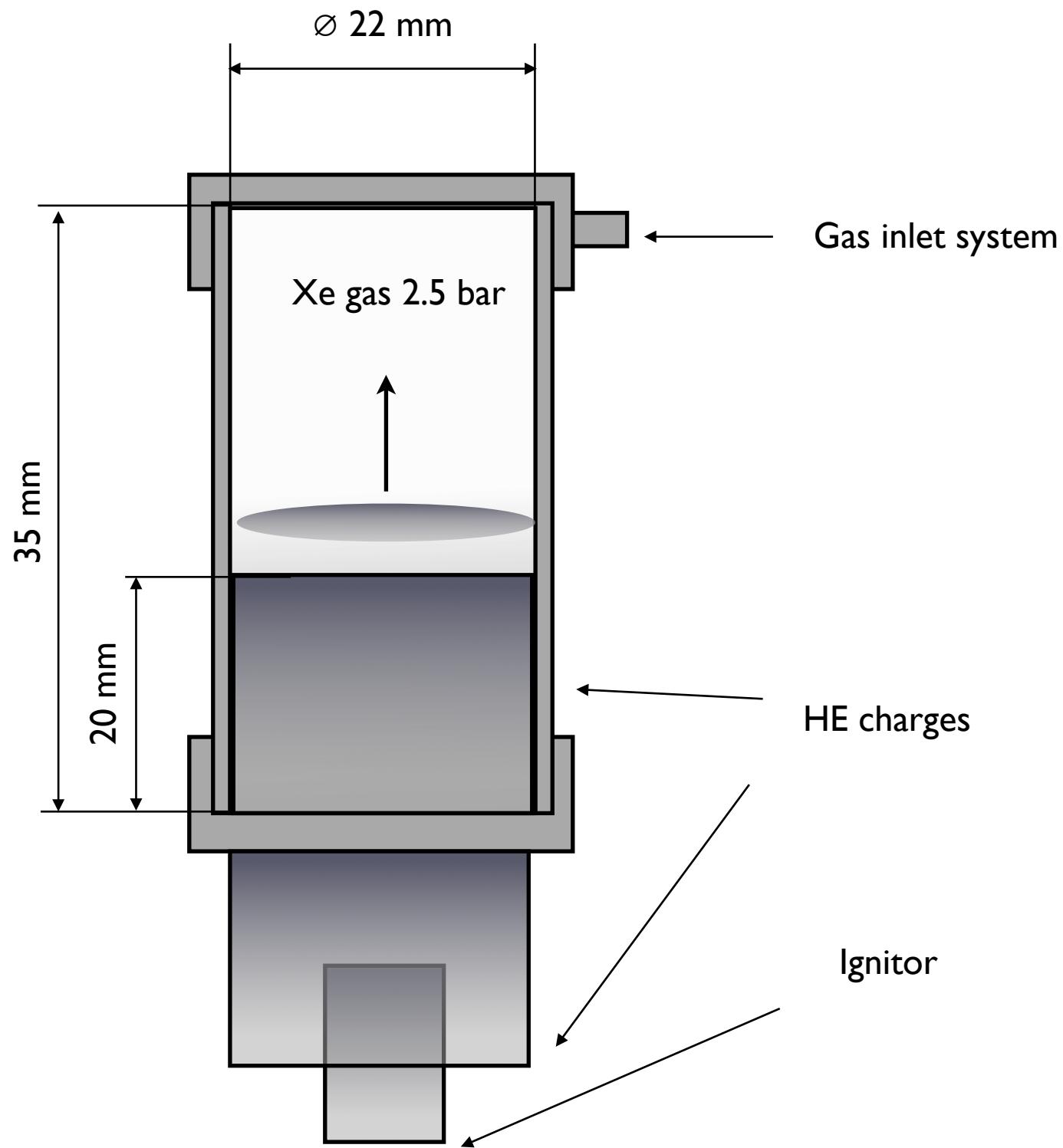


Velocity of the free surface:
1.68 km/s

Velocity of the head of the jet:
4 km/s

Shock Compression of Noble Gases

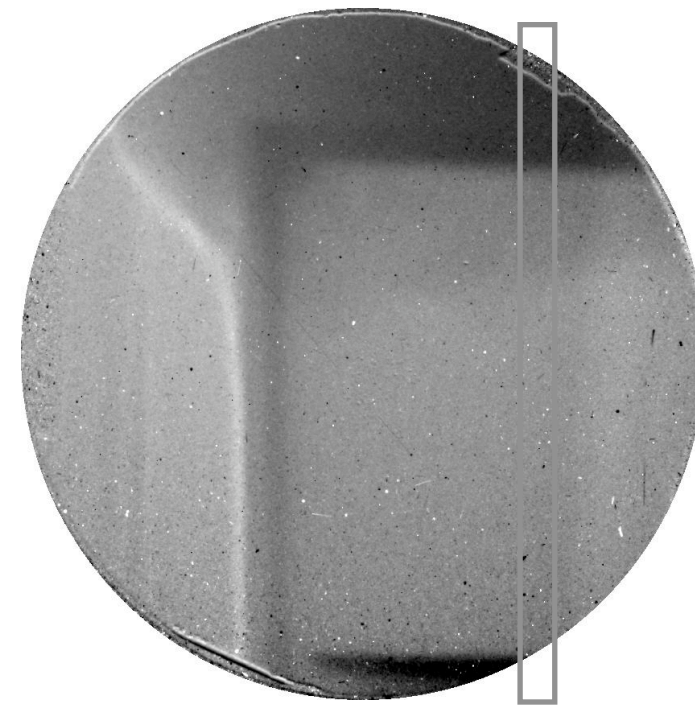
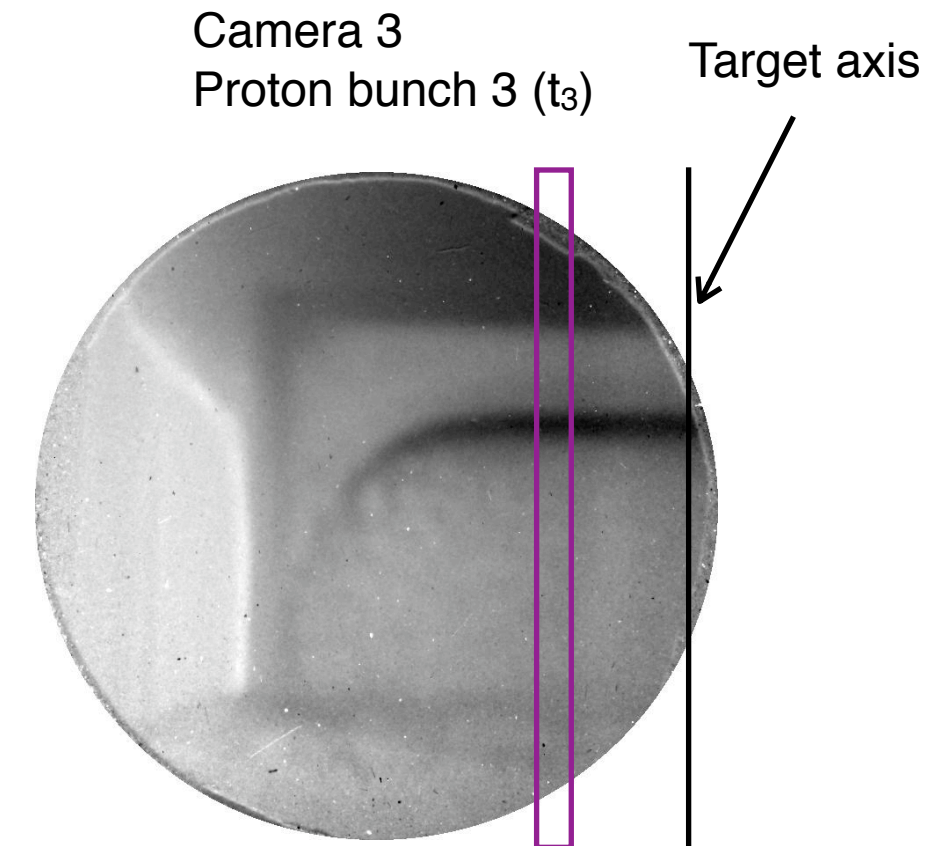
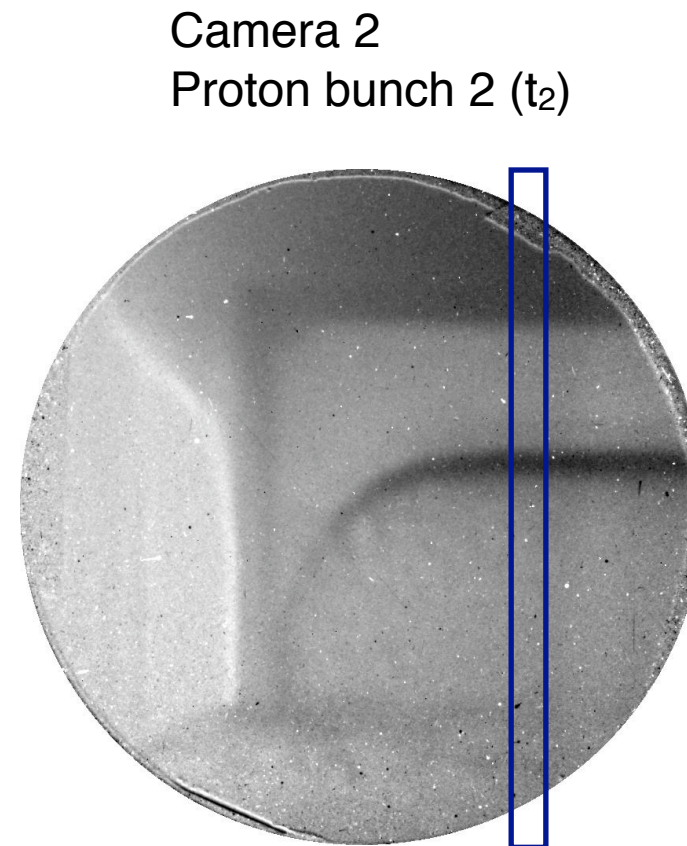
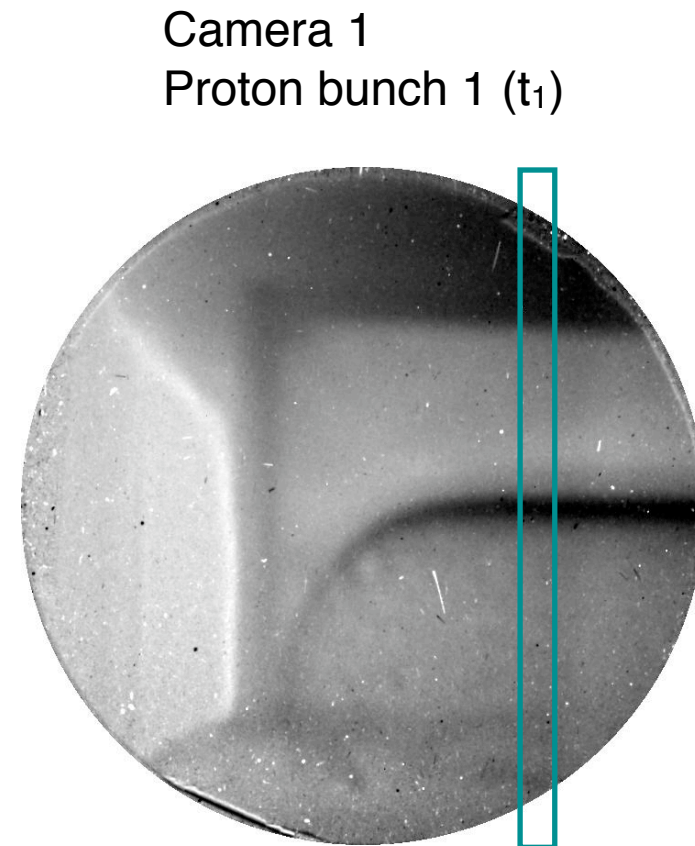
Target scheme



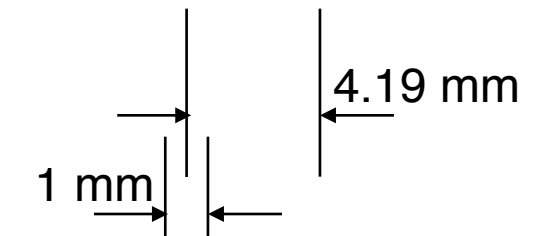
Target photo



Shock Compression of Noble Gases



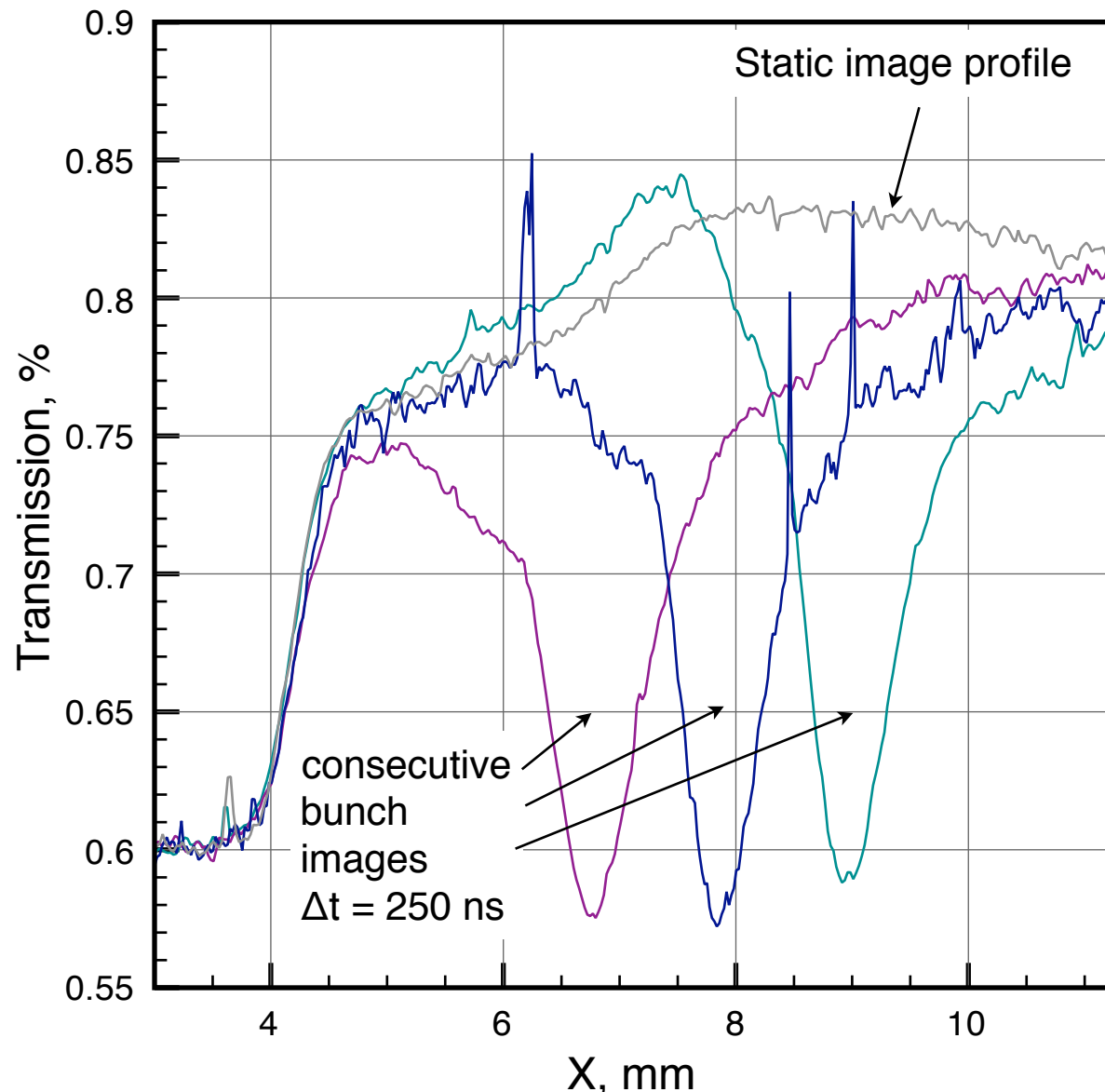
$\Delta t = t_2 - t_1 = t_3 - t_2 = 250 \text{ ns}$
 $\delta t(\text{FWHM}) = 70 \text{ ns}$



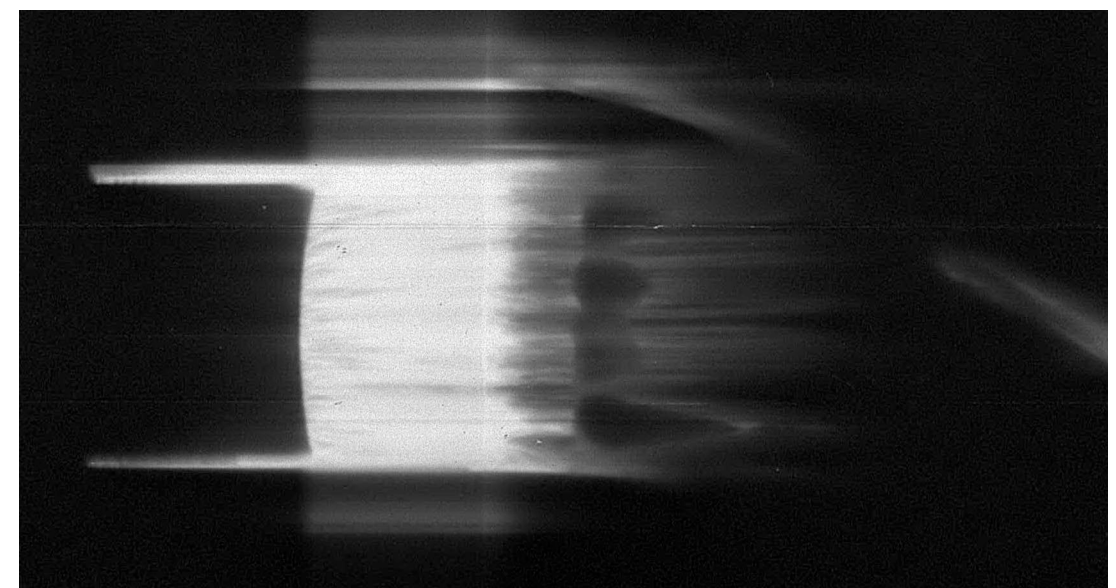
Gas cell thickness - 20.34 mm
Gas pressure - 2.5 Bar
 $\rho_0 = 2.5 * 2.034 * 0.00589 = 0.03 \text{ g/cm}^2$

Shock Compression of Noble Gases

Beam transmission for image profiles



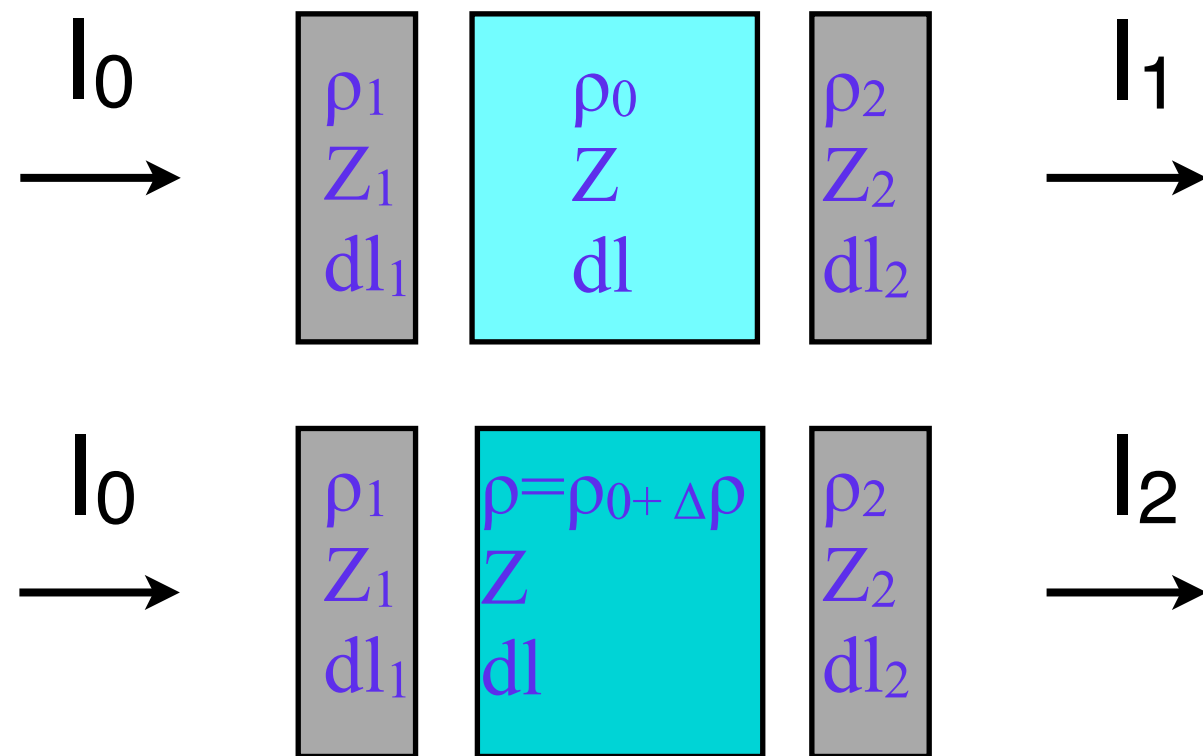
SFR image



$$U = 4.3 \pm 0.2 \text{ km/s}$$

Shock Compression of Noble Gases

Beam transmission for composite target



$$T1 = I_1/I_0 = T(\rho_1, Z_1, dl_1) * T(\rho_0, Z, dl) * T(\rho_2, Z_2, dl_2)$$

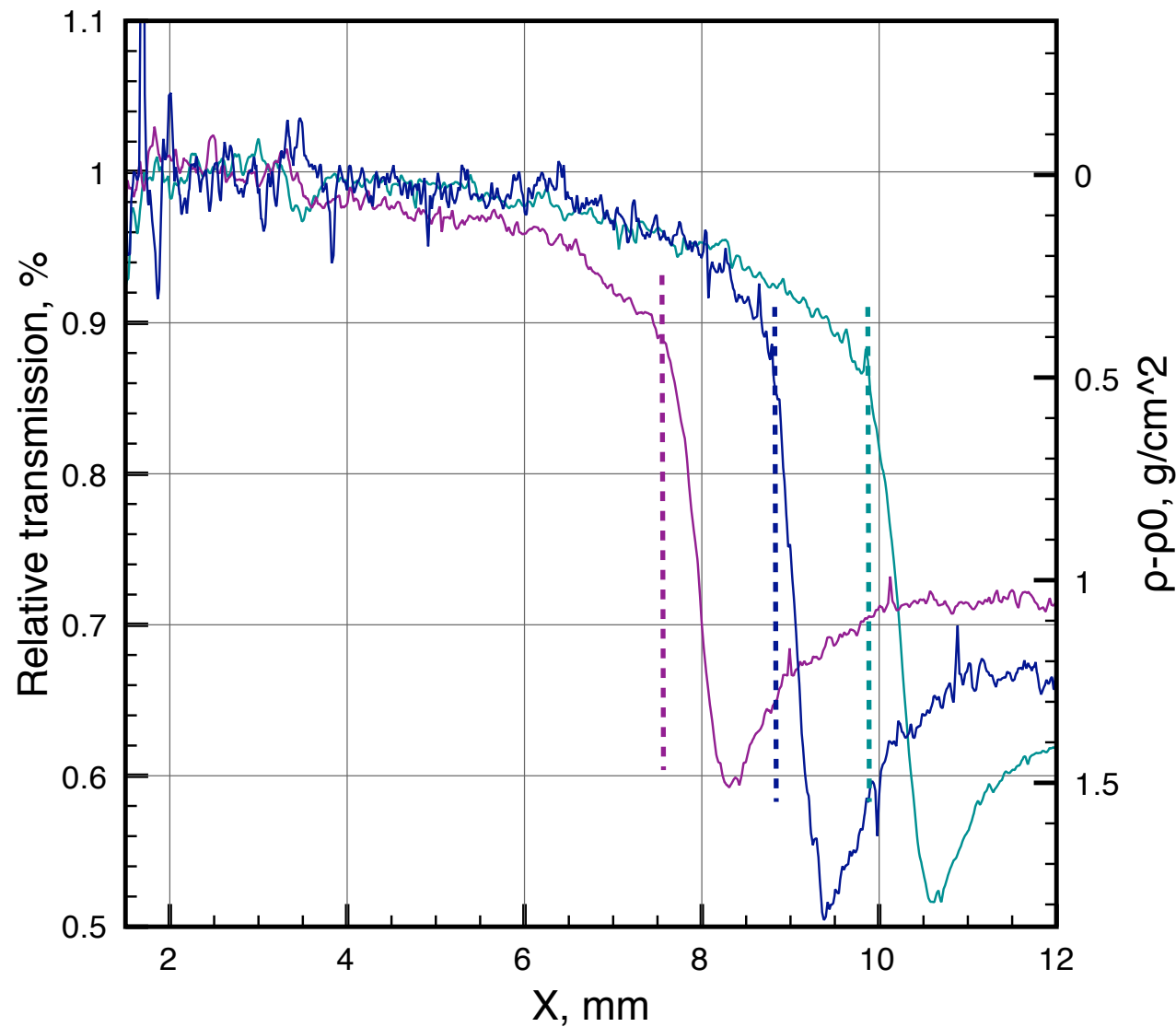
$$\begin{aligned} T2 = I_2/I_0 &= T(\rho_1, Z_1, dl_1) * T(\rho, Z, dl) * T(\rho_2, Z_2, dl_2) = \\ &= T(\rho_1, Z_1, dl_1) * T(\rho_0, Z, dl) * T(\Delta\rho, Z, dl) * T(\rho_2, Z_2, dl_2) \end{aligned}$$

$$T2/T1 = T(\Delta\rho, Z, dl)$$

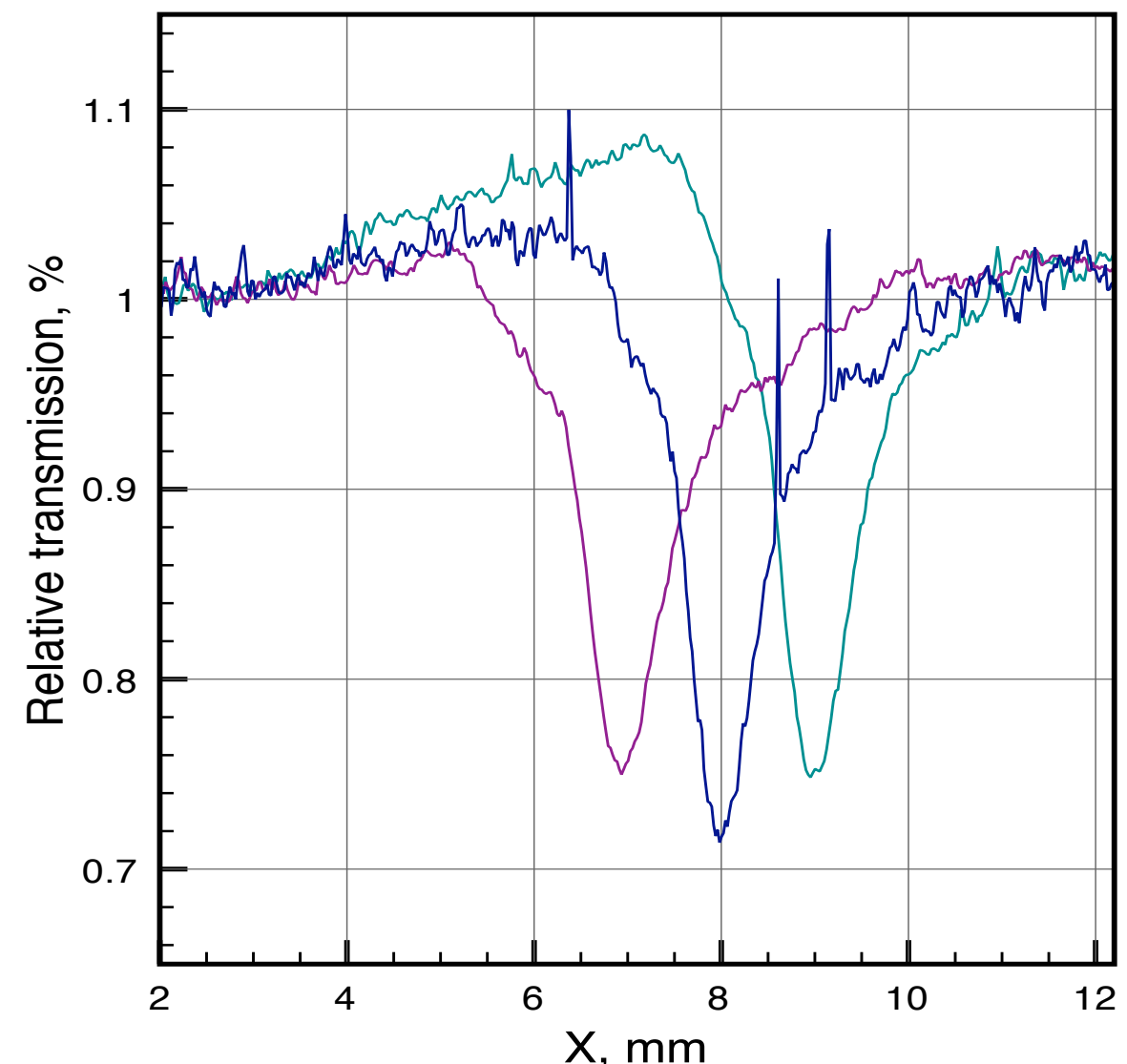
Shock Compression of Noble Gases

Beam transmission for image profiles (relative to static image)

Ar gas 3.5 Bar



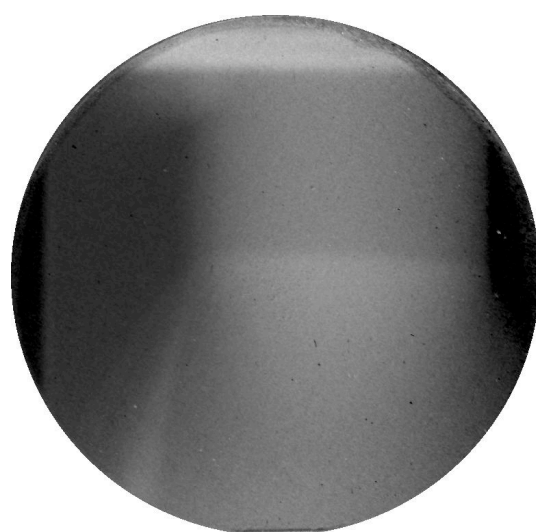
Xe gas 2.5 Bar



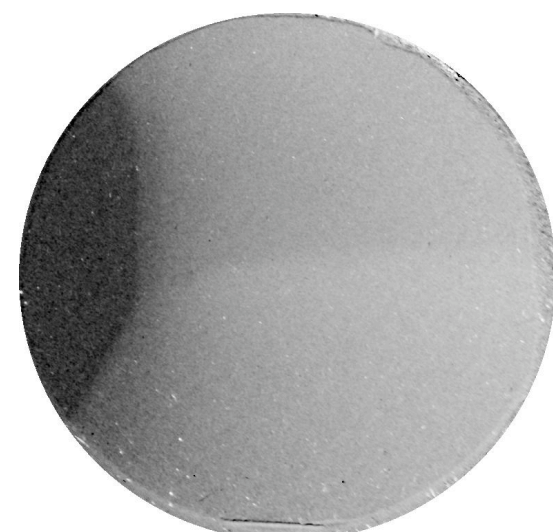
Proton Radiography of Dense Plasma

Under investigation on ITEP Proton Microscope setup:

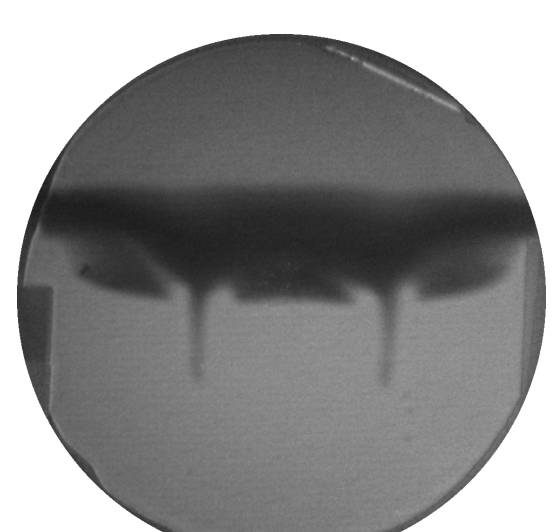
- Detonation of pressed TNT charge
- Detonation of Emulsion Explosive
- Dynamic Fracture and Surface Ejecta Formation
- Shock Compression of Noble Gases



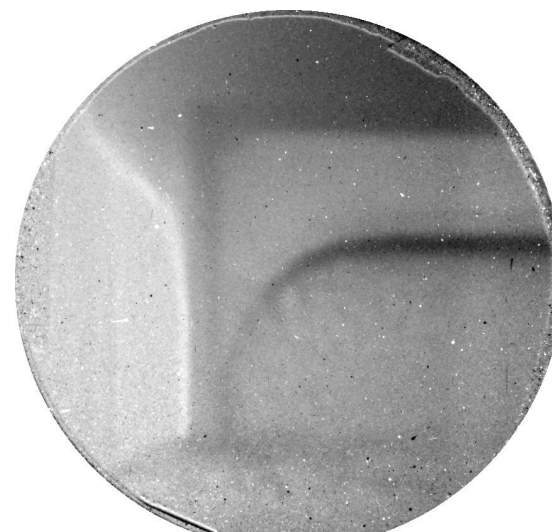
TNT
detonation



EHE
detonation



Ejecta
formation



Gas
shock compression

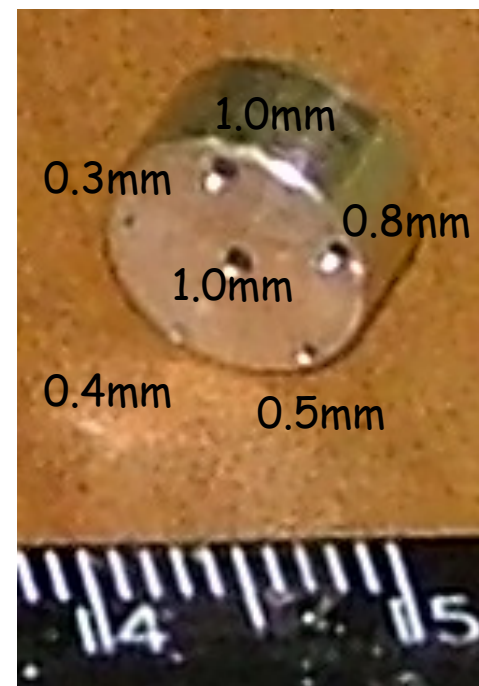
ITEP Proton Microscope: Static test-objects

Tomography reconstruction of multi-projection proton microscopy

Targets and SS container



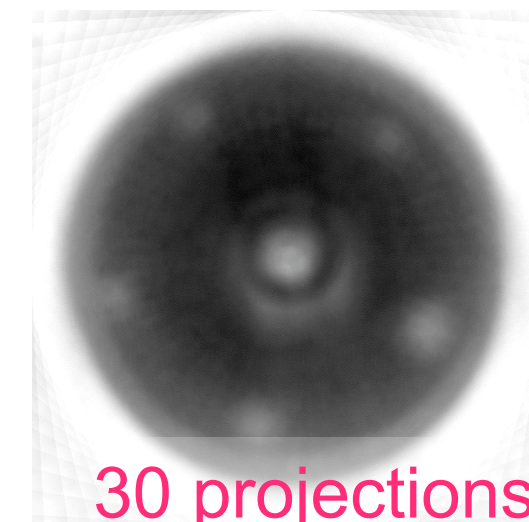
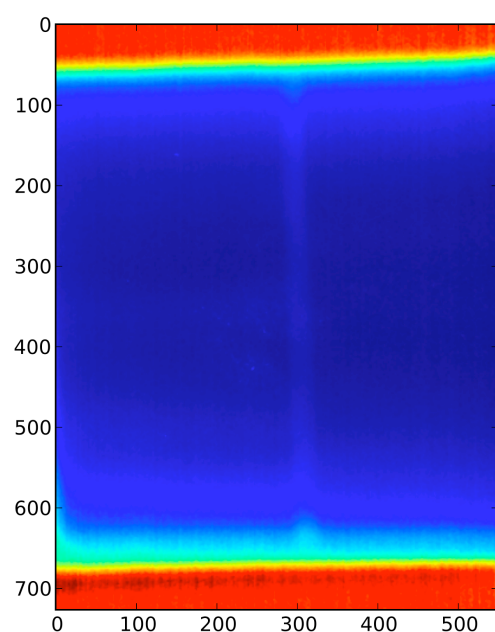
Brass target



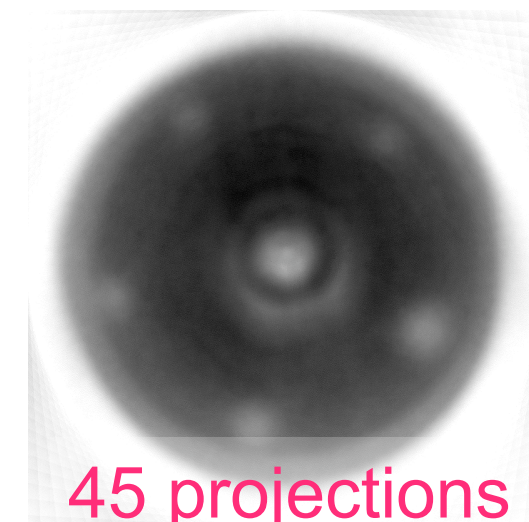
Requirements:

- good spatial and density resolution for projection images
- high precision for target positioning and alignment

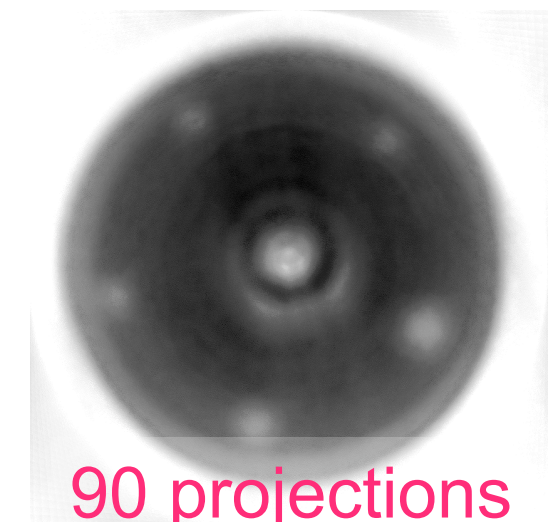
Reconstructed two-dimensional target density distribution by Algebraic Reconstruction Technique (ART)



30 projections

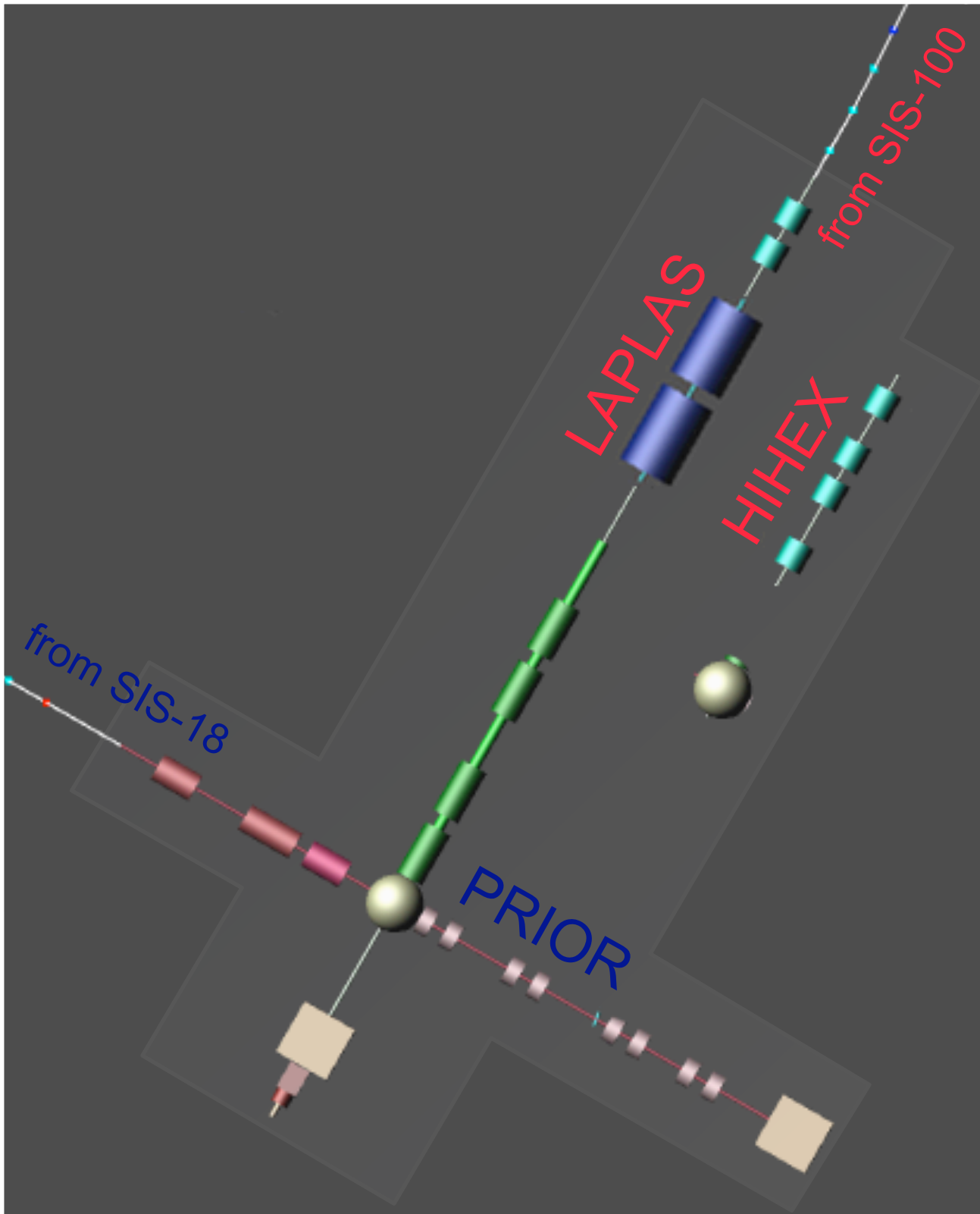


45 projections



90 projections

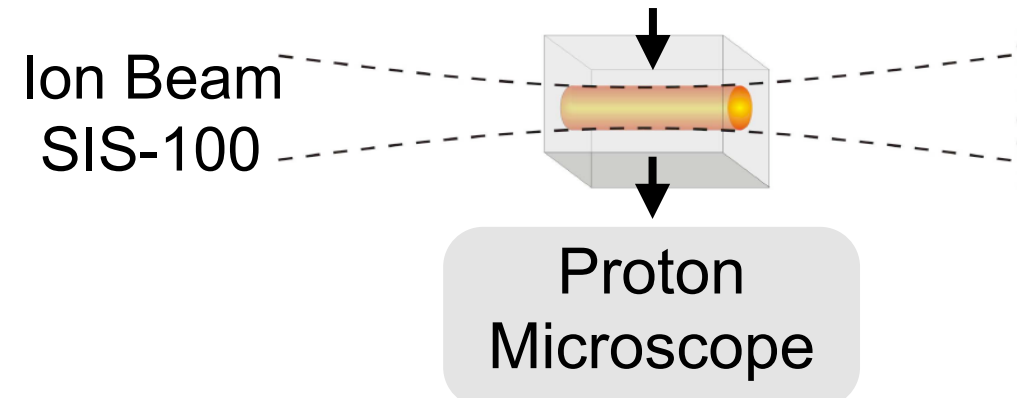
Plasma Physics beam lines and cave at FAIR



SIS-18:

a dedicated radiography beam line -
density diagnostics for
LAPLAS and **HIHEX** experiments

Proton Beam SIS-18



PRIOR - Proton Microscope for FAIR:

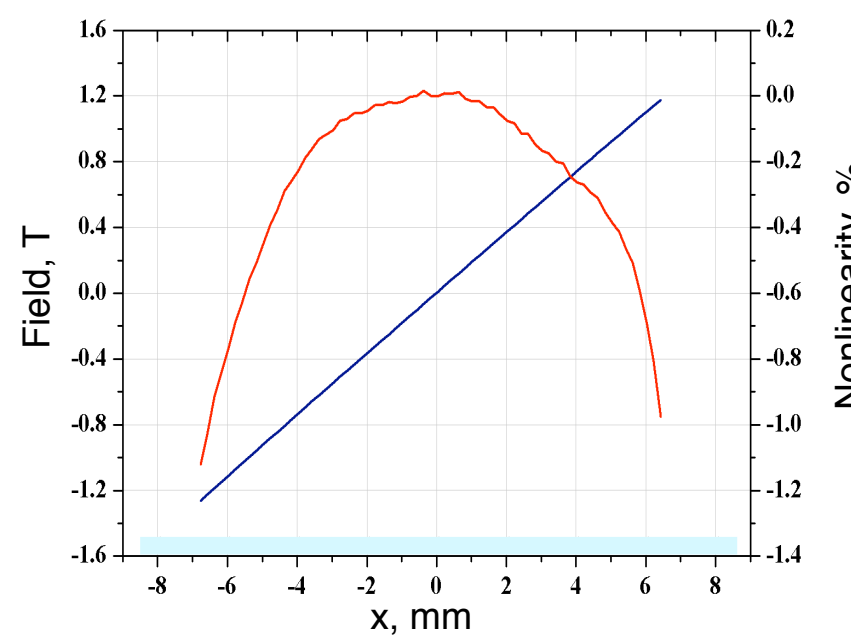
- proton energy **4.5 GeV**
- up to **~20 g/cm²** (Fe, Pb, Au, etc.)
- **≤10 μm** spatial resolution
- **10 ns** time resolution (multi-frame)
- **sub-percent** density resolution
- proton illumination spot size: **3–15 mm**
- imaging, aberrations correction by magnets

Permanent Magnetic Quadrupoles (PMQ) - prototype manufacturing

High Gradient
Split-Pole Quadrupole



High Gradient
Split-Pole Quadrupole



Hall Probe
Measurement Bench



- Pole field: ~ 1.6 T
- Final gradient: 211.6 T/m
- Nonlinearity: < 0.9 %
- Two layers with circular 16 sectors
- NdFeB alloy with coercivity on magnetization of 2.7 T in the inner layer of 43 mm diameter

Permanent Magnetic Quadrupoles (PMQ) - final design for PRIOR

2 x PMQ L = 165 mm

2 x PMQ L = 330 mm

All quads have the same cross-section

All quads are of three layers

Each layer contains 24 magnetic elements of prismatic shape. Angle size of all magnetic elements – 15°

All quads are divided longitudinally by modules of the same length of 33 mm. Total number of modules – 30.

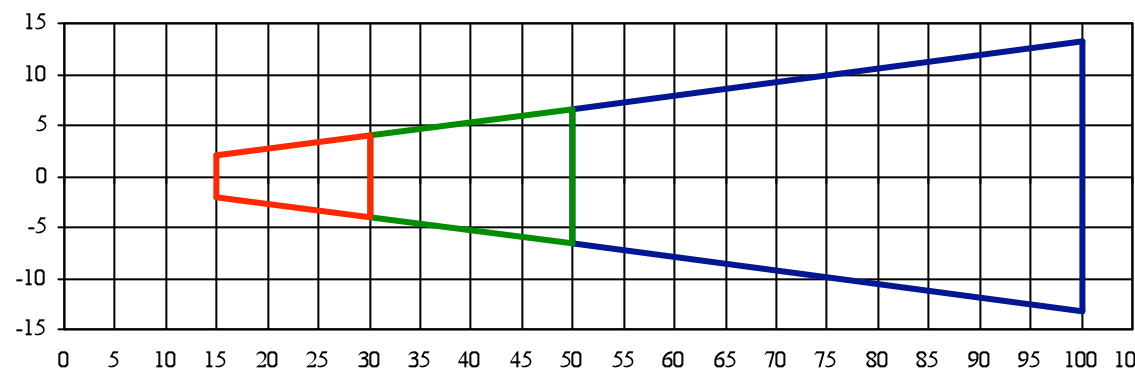


Figure 1. Cross-sections of prismatic elements for three-layer modules.

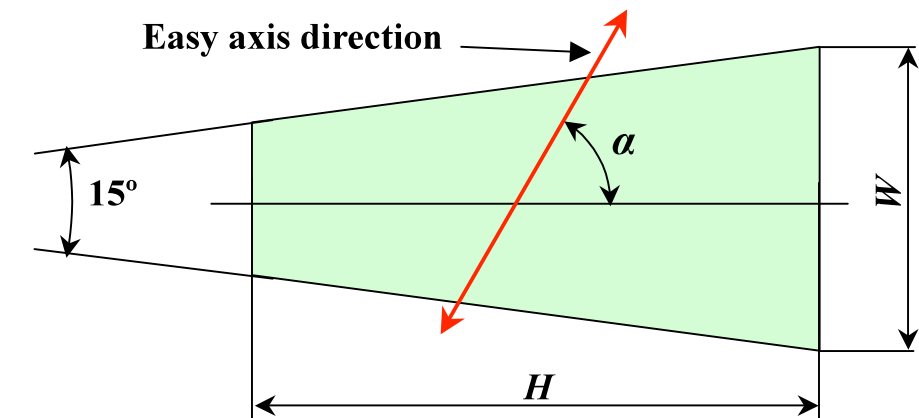


Figure 2. Cross-section parameters of prismatic elements and easy axis slope to the prism's plane of symmetry for three-layer quads

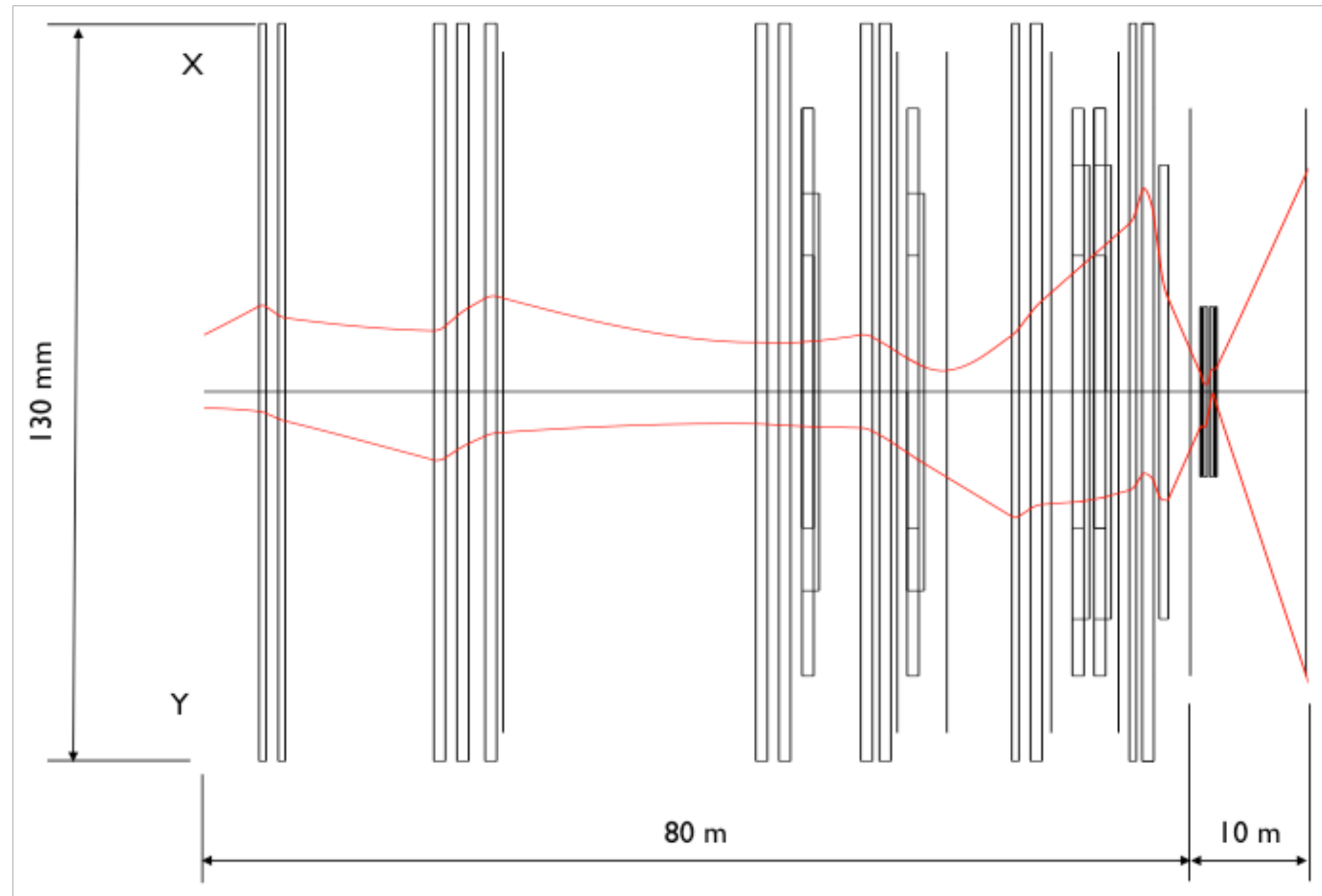
Table 1. Segments dimensions for each layer

	Layer №1 Alloy VACODYM 863 TP: Br=1.27 T, $\mu_0 \cdot HCJ=2.7$ T	Layer №2 Alloy VACODYM 854 TP: Br=1.32 T, $\mu_0 \cdot HCJ=2.2$ T	Layer №2 Alloy VACODYM 745 TP: Br=1.40 T, $\mu_0 \cdot HCJ=1.4$ T
Segment sizes, W x H x L, mm	$8^{+0.1} \times 15^{+0.2} \times 33^{+0.1}$	$13.2^{+0.1} \times 20^{+0.2} \times 33^{+0.1}$	$26.5^{+0.1} \times 50^{+0.2} \times 33^{+0.1}$

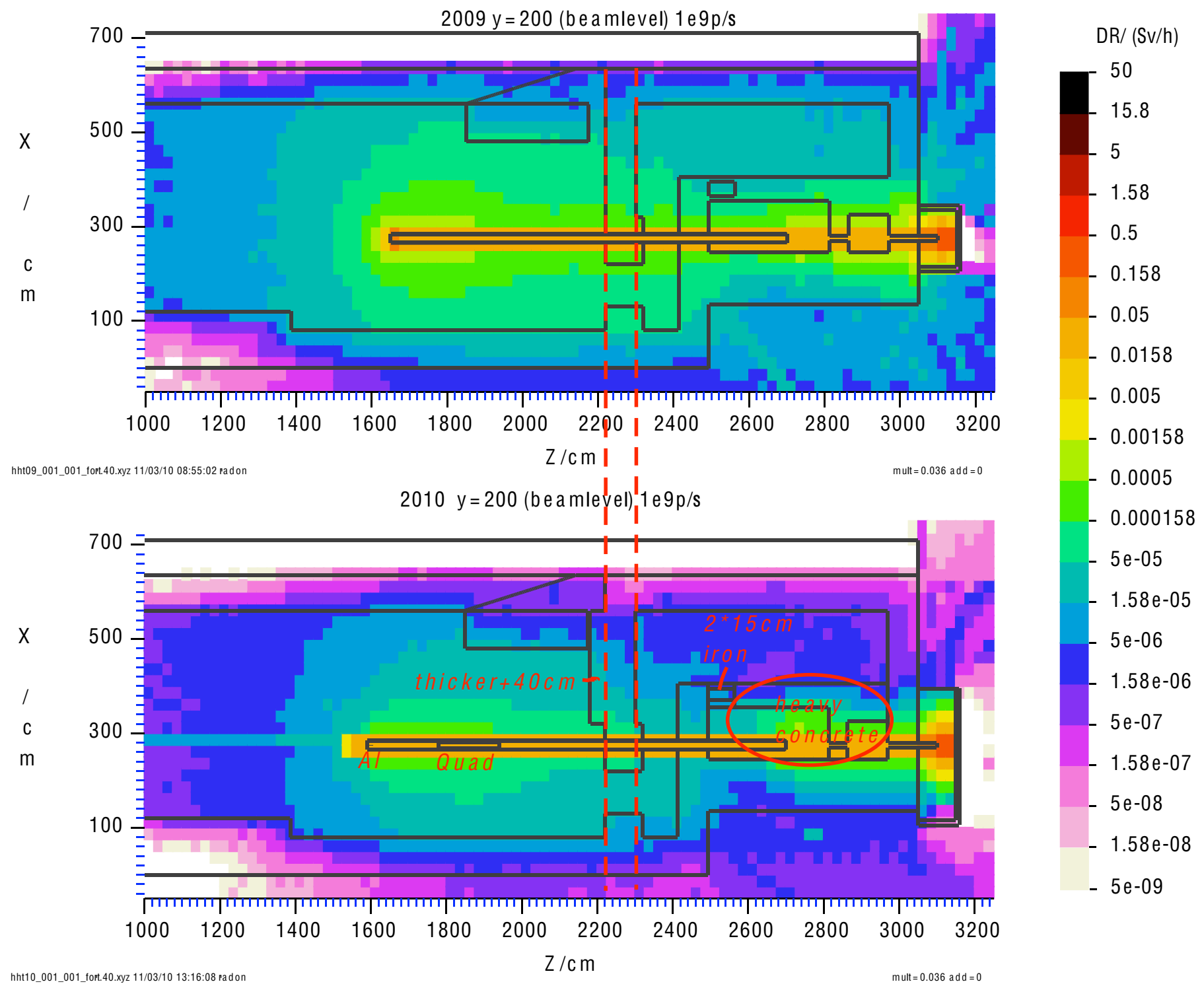
Table 2. Types of segments on easy axis slope

	Type №1	Type №2	Type №3
α	15°	45°	75°

HHT beam line matching to PRIOR optics



HHT beam line FLUKA simulation



HHT beam line FLUKA simulation

